# Conformational Closure of the Catalytic Site of Human CD38 Induced by Calcium[†,‡]

Qun Liu,[§] Richard Graeff,[||] Irina A. Kriksunov,[§] Connie M. C. Lam,[⊥] Hon Cheung Lee,*[,||,⊥] and Quan Hao*[,§,⊥,#]

*MacCHESS, Cornell High Energy Synchrotron Source, and School of Applied and Engineering Physics, Cornell University, Ithaca, New York 14853, Department of Pharmacology, University of Minnesota, Minneapolis, Minnesota 55455, and Department of Physiology, University of Hong Kong, Hong Kong, China*

*Received August 29, 2008; Revised Manuscript Received November 10, 2008*

ABSTRACT: First identified on the surface of lymphoids as a type II transmembrane protein, CD38 has now been established to have dual functions not only as a receptor but also as a multifunctional enzyme, catalyzing the synthesis of and hydrolysis of a general calcium messenger molecule, cyclic ADP-ribose (cADPR). The receptorial functions of CD38 include the induction of cell adhesion, differentiation, apoptosis, and cytokine production upon antibody ligation. Here we determined the crystal structure of calcium-loaded human CD38 at 1.45 Å resolution which reveals that CD38 undergoes dramatic structural changes to an inhibited conformation in the presence of calcium. The structural changes are highly localized and occur in only two regions. The first region is part of the active site and consists of residues 121−141. In the presence of calcium, W125 moves 5 Å into the active site and forms hydrophobic interactions with W189. The movement closes the active site pocket and reduces entry of substrates, resulting in inhibition of the enzymatic activity. The structural role of calcium in inducing these conformational changes is readily visualized in the crystal structure. The other region that undergoes calcium-induced changes is at the receptor region, where a highly ordered helix is unraveled to a random coil. The results suggest a novel conformational coupling mechanism, whereby protein interaction targeted at the receptor region can effectively regulate the enzymatic activity of CD38.

Human CD38 is a type II transmembrane protein, containing a short amino-terminal tail, a single transmembrane helix, and a large ectoenzyme portion (*1*). The ectoenzyme portion (residues 45−300) can catalyze multiple reactions, including the formation of cyclic ADP-ribose (cADPR)[1] and ADP-ribose from NAD (*2*), synthesis of nicotinic acid adenine dinucleotide phosphate (NAADP) from NADP and nicotinic acid by a base-exchange reaction (*3, 4*), and hydrolysis of cADPR and NAADP (*2, 5*). Both cADPR and NAADP mobilize intracellular calcium stores (*6, 7*). ADP-ribose, the hydrolysis product of cADPR, is itself a signaling molecule that activates the TRPM2 calcium channel and induces calcium influx across the plasma membrane in a cADPR or NAADP synergized manner (*8*−*10*). The crystal structure of this ectoenzyme reveals two domains: the α-helix-rich N-domain comprising residues 45−118 and 144−200 and the β-strand-rich C-domain comprising residues 119−143 and 201−300 (*11*). CD38-catalyzed reactions take place in a unique active site pocket defined by residues E226, S193, E146, W125, R127, W189, and D155 (*12*−*14*) and located between two domains. Structural determinants for the production and hydrolysis of these calcium-mobilizing molecules have been elaborated recently (*5, 12, 15, 16*).

Human CD38 expressed on the surface of lymphocytes adopts a topology so that its enzymatic domain is extracellular with its short amino tail in the cytosol. It is known that structural modifications induced by exogenous (soluble factors, drugs, etc.) or internal (activation, differentiation, etc.) events may be followed by structural modifications of cell surface molecules. Out of these, ligation with agonistic monoclonal antibodies (mAbs) is a model adopted to recapitulate in vitro the complexity of the modifications observed in vivo. Antigenic ligation of the enzymatic domain of CD38 by agonistic mAbs can induce a variety of cellular changes, including cell adhesion, apoptosis, lymphopoiesis, and cytokine production (*17*). CD31, an adhesion molecule with an immunoglobulin topology, has been proposed as a physiological ligand of CD38. The interaction between CD38 and CD31 has been suggested to be important for lymphocyte adhesion in a human endothelial cell (*18*). In human monocytes, the ligation of CD38 by either CD31 or agonistic mAbs induces the expression of the same cytokines (*19*). In fact, in T lymphocytes, most functions attributed to the ligation of CD38 by its agonistic antibodies can be reproduced by the ligation of CD38 with CD31 (*18*). The receptor

[†] This work was supported by grants from the NIH to MacCHESS (RR01646) and H.C.L./Q.H. (GM061568) and by RGC Grant HKU-769107M.

[‡] Coordinates have been deposited in the Protein Data Bank as entry 3F6Y.

* Corresponding authors. H.C.L.: tel, 852-2819-9163; fax, 852-2817-1334; e-mail, leehc@hku.hk. Q.H.: tel, 852-2819-9194; fax, 852-2855-9730; e-mail, qhao@hku.hk.

[§] MacCHESS, Cornell High Energy Synchrotron Source, Cornell University.

[||] University of Minnesota.

[⊥] University of Hong Kong.

[#] School of Applied and Engineering Physics, Cornell University.

[1] Abbreviations: NAD, nicotinamide adenine dinucleotide; cADPR, cyclic ADP-ribose; NAADP, nicotinic acid adenine dinucleotide phosphate; ADPR, ADP-ribose.

10.1021/bi801642q CCC: $40.75 
Published on Web 12/08/2008

region on human CD38 targeted by the mAbs has been mapped to the enzymatic domain and includes carboxyl-terminal residues 273−285 (*20, 21*).

That both the enzymatic and receptorial functions are physically localized to the same extracellular portion of CD38 suggests that the two functions could be structurally coupled. Indeed, it has been shown that truncation of the receptor region consisting of the 28 residues (273−300) at its carboxyl terminus of CD38 also abrogated its NADase activity, strongly indicating its importance in both the enzymatic and receptorial functions of the molecule (*20*). Recently, ligation of CD38 by two mAbs, CS/2 and clone 90, was found to affect CD38's NAD hydrolyase activity, providing further evidence of correlation between its receptorial and enzymatic functions (*22*). Although prior experiments implied structural changes in CD38 during the coupling events (*23*), it is unclear how both functions are structurally correlated as the receptor region is far away from the catalytic site (*11*). Besides mAbs, other modifiers, including metal ions, can also be adopted to induce structural modifications for functional studies even before knowing their exact biological functions. Metal ions have been shown to regulate CD38's enzymatic activities and are correlated with detectable conformational changes (*24*). Calcium is also a metal ion, and its flux can be physiologically triggered by cADPR, the enzymatic product of CD38. Therefore, it would be of interest to investigate the ability of calcium to modify CD38's enzymatic and receptorial functions, with a goal to recapitulate unknown functions of CD38 in vivo. In this study, we show by crystallography that calcium can bind to CD38 and induce conformational changes, resulting in closure of the catalytic site and disorder of the receptor. Our results suggest a novel conformational coupling mechanism between the enzymatic and receptorial functions of the molecule.

## EXPERIMENTAL PROCEDURES

*Protein Production, Crystallization, and Data Collection.* The wild-type CD38 sample was produced with procedures reported previously (*13*). To obtain the calcium-loaded structure, 100 mM calcium chloride was added into the crystallization precipitants. The crystal was obtained by a hanging-drop vapor diffusion method. The crystallization mother liquor contains 10% PEG 4000, 100 mM MES, pH 7.5, and 100 mM calcium chloride. It took about 10 days to form crystals with sizes suitable for data collection. One complete data set to 1.45 Å resolution was collected at the CHESS A1 station under the protection of a liquid nitrogen cryostream at 100 K. Raw images were integrated, scaled, and merged by using the program HKL2000 (*25*). Crystallographic statistics for this data set are listed in Table 1.

*Structure Determination and Refinement.* The crystal belongs to space group *C*2. The solvent content estimation shows that there is only one CD38 molecule in the crystallographic asymmetric unit. Initial efforts to solve the *C*2 form structure by molecular replacement with the previously determined calcium-free structure (PDB ID 1YH3) were not successful. It was then realized that the calcium-loaded structure might be very different from that of the calcium-free structure. Calcium-free CD38 has two domains: N-domain and C-domain. With the assumption that the structural changes could be domain-dependent, the model was disassembled into two pieces, each containing one domain. Each domain was used as a search model for the molecular replacement with the program MOLREP (*26*). Only the N-term domain resulted in a solution from which the derived model can be refined with a decreasing free *R* factor. After the preliminary refinement of the partial model in REFMAC5 (*27*), the *R* and $R_{free}$ factors were 0.43 and 0.48, respectively. Program Arp/Warp (*28*) was used to update the model to obtain improved electron density for the whole calcium-loaded structure. The C-domain model was then built in O (*29*) with the guidance of the improved electron density and calcium-free CD38 model. Three very high peaks (>10 $\sigma$) in the difference electron density maps with coefficients $F_o - F_c$ were modeled as calcium ions. All subsequent isotropic and anisotropic refinements were carried out in REFMAC5. Structural refinement and model statistics are also listed in Table 1.

Table 1: Crystallographic Data, Refinement, and Model Statistics[a]

| | |
|---|---|
| **Data Collection** | |
| cell dimensions | |
| *a*, *b*, *c* (Å) | 84.69, 60.06, 56.93 |
| α, *β*, *γ* (deg) | 90.00, 129.69, 90.00 |
| space group | *C*2 |
| resolution (Å) | 30−1.45 (1.50−1.45) |
| unique reflections | 35690 |
| multiplicity | 3.3 (1.7) |
| $I/\sigma$ | 25.28 (2.08) |
| $R_{merge}$ (%) | 4.4 (32.6) |
| completeness (%) | 91.5 (52.6) |
| **Refinement** | |
| resolution (Å) | 20−1.45 |
| *R* factor (%) | 14.62 |
| $R_{free}$ factor (%) | 18.41 |
| protein atoms | 1860 |
| water molecules | 286 |
| calcium ions | 3 |
| mean *B* (Å$^2$) | 21.36 |
| rms deviations | |
| bond lengths (Å) | 0.01 |
| bond angles (deg) | 1.33 |
| Ramachandran plot | |
| most favored (%) | 93.1 |
| additional allowed (%) | 6.4 |
| generally allowed (%) | 0.5 |
| disallowed (%) | 0.0 |

[a] Values in parentheses are from the highest resolution shell. $R_{merge} = \sum|I - \langle I\rangle|/\sum I$, where *I* is the integrated intensity of a given reflection. $R = \sum||F_o| - |F_c||/\sum|F_o|$. $R_{free}$ was calculated using 5% of data excluded from refinement.

*NADase Assay.* CD38 (30−80 ng/mL) was incubated with various concentrations of NAD (2−200 $\mu$M) at 20−23 °C for 3−20 min in a medium containing 25−50 mM HEPES, pH 7.0. The reaction was stopped by addition of 150 mM HCl. After neutralization with 0.35 M phosphate buffer (pH 8.0), aliquots of the reaction mixture were diluted into a fluorometric cycling assay medium for NAD as described previously (*30*) and the amounts of NAD remaining in the reaction mixture determined. Where indicated, $CaCl_2$ (0−100 mM) was included in the CD38 reaction medium to assess the effect of calcium on the NADase activity of CD38.

## RESULTS

*Structure Determination of Calcium-Loaded CD38.* To determine whether CD38 can load calcium, we first tried to soak preformed CD38 crystals with various concentrations of calcium chloride at room temperature. This was not

successful, and no clear calcium peaks were seen in the $F_o - F_c$ difference electron density maps (data not shown). It is likely that the crystal lattice of the preformed crystal prevented the binding of calcium ions. We then tried to cocrystallize calcium with CD38. After screening and optimization, crystals were obtained in the presence of 50 mM calcium and pH 7.5. The crystals diffracted quite well, and we were able to collect diffraction data up to 1.45 Å resolution. Initial molecular-replacement trials to solve the structure using the calcium-free structure (PDB ID 1YH3) failed, suggesting significant conformational changes between the calcium-loaded and calcium-free structures. The calcium-free structure consists of the α-helix-rich N-domain and the β-strand-rich C-domain (*11*). With the assumption that domain−domain movement may result in conformational changes, the search model was split into two domains. The calcium-loaded structure was then determined from the N-domain partial model by molecular replacement.

*Conformational Changes between the "Off" and "On" Structures.* The calcium-loaded structure was refined at a resolution of 1.45 Å (Figure 1A). The refined structure contains residues 45−279 with the C-terminal tail (residues 280−300) disordered. The calcium-loaded structure contains two domains, the N-domain and C-domain. The active site residues, including W125, E146, D155, W189, and S193, reside between the two domains. The most significant structural feature of the calcium-loaded structure is the close stacking of residues W125 and W189, two door-keeping residues of the active site, resulting in the closure of the catalytic site (Figure 1A). Therefore, the calcium-loaded structure will be called the "off" conformation, while the calcium-free structure will be called the "on" conformation. Alignment of the "off" and "on" structures is shown in Figure 1B. The rms deviation for 230 Cα atoms (residues 50−279) is 2.09 Å. The two structures have almost identical N-domains, suggesting that the N-domain is invariable during the loading of calcium. However, significant structural changes for the C-domain were observed following binding of calcium (Figure 1B). The largest structural changes were observed in two regions of the C-domain of the "off" structure. The first one consists of the disorder of the carboxyl tail (residues 280−300) (Figure 1B,C), which has previously been identified as the receptor region for several monoclonal antibodies (*20*). In the "on" structure, this receptor region consisted of a highly ordered helix with only the last four residues as a disordered coil (Figure 1B, purple and labeled receptor), while in the "off" structure, the helix was destabilized and totally disordered in the last 21 residues. The second major structural change is near the active site and includes residues 121−141. In the "on" structure, the conformation of residues 121−141 was such that the active site pocket was fully open, allowing the entry and binding of the substrate, such as NAD (labeled V-open, colored orange, Figure 1C, right panel). In the "off" structure, the movement of residues 121−141 from its orange conformation to the green conformation (labeled V-close, colored green) occluded the active site (Figure 1C, left panel). It has previously been shown that the "on" structures, whether complexed with substrates/products (NAD, cADPR, ADPR) or in the apo form, have very similar active site structures (*12, 15*). The dramatic structural changes induced by calcium, leading to the closure of the active site, are thus highly remarkable.

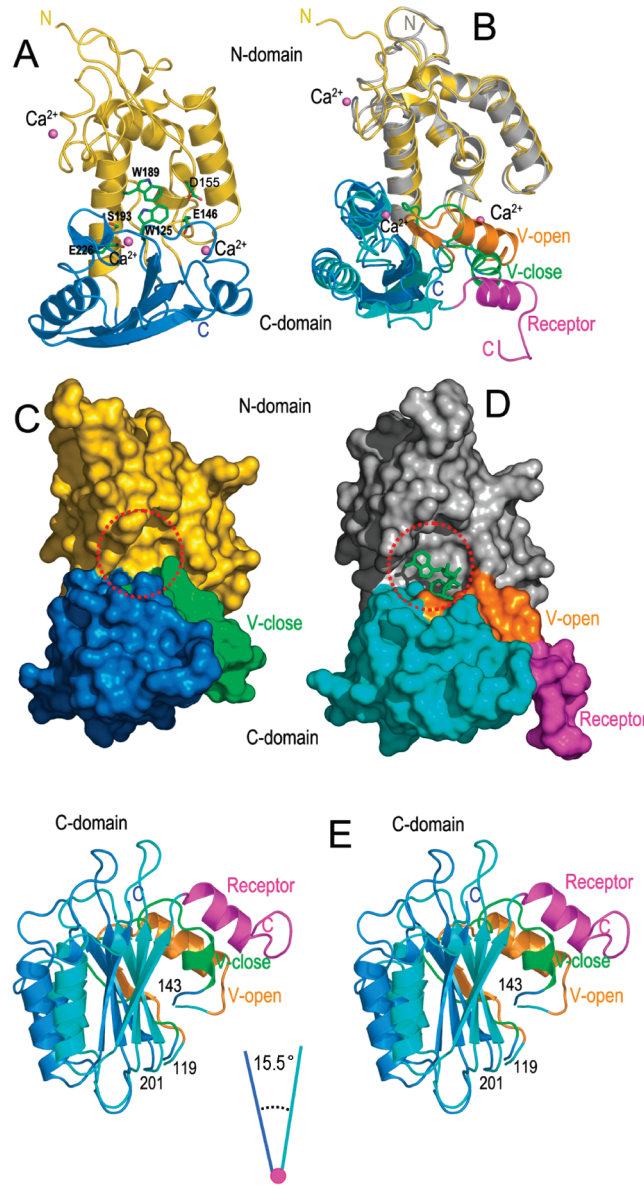


FIGURE 1: Structure of calcium-loaded CD38. (A) Ribbon view of the overall structure of calcium-loaded CD38. The N-domain (yellow) and C-domain (marine) are separately colored. The catalytic site is located between two domains. Residues in the catalytic site critical for the enzymatic activities of CD38 are shown as green sticks. (B) Comparison of the calcium-loaded structure ("off") with the calcium-free structure ("on") of CD38. The "on" and "off" structures are aligned against their N-domains. The receptor region in the "on" structure is colored in magenta and consists of a helix, while in the "off" structure, this receptor region is disordered. The region of residues 121−141 is also adopting very different conformations and thus is labeled as V-open in the "on" structure and V-close in the "off" structures. (C) and (D) are surface representations of the "off" (C) and "on" structures (D). The color scheme of (C) and (D) is the same as that of (B). Dashed red circles highlight the active sites in "off" (C) and "on" (D) structures. Substrate NAD is shown as green sticks in the active site of the "on" structure. (E) Stereoview showing that the C-domains of the "off" (marine and green) and "on" (cyan, orange, and magenta) structures are related by a rotation of 15.5°.

Besides these conformational changes between "on" and "off" structures, there exists a relative domain−domain rotation after the loading of calcium as shown in Figure 1E. With their N-domains aligned as shown in Figure 1B, it can be seen that the segment containing residues 201−279 is shifted by a rotation (Figure 1E). Indeed, if the segment in

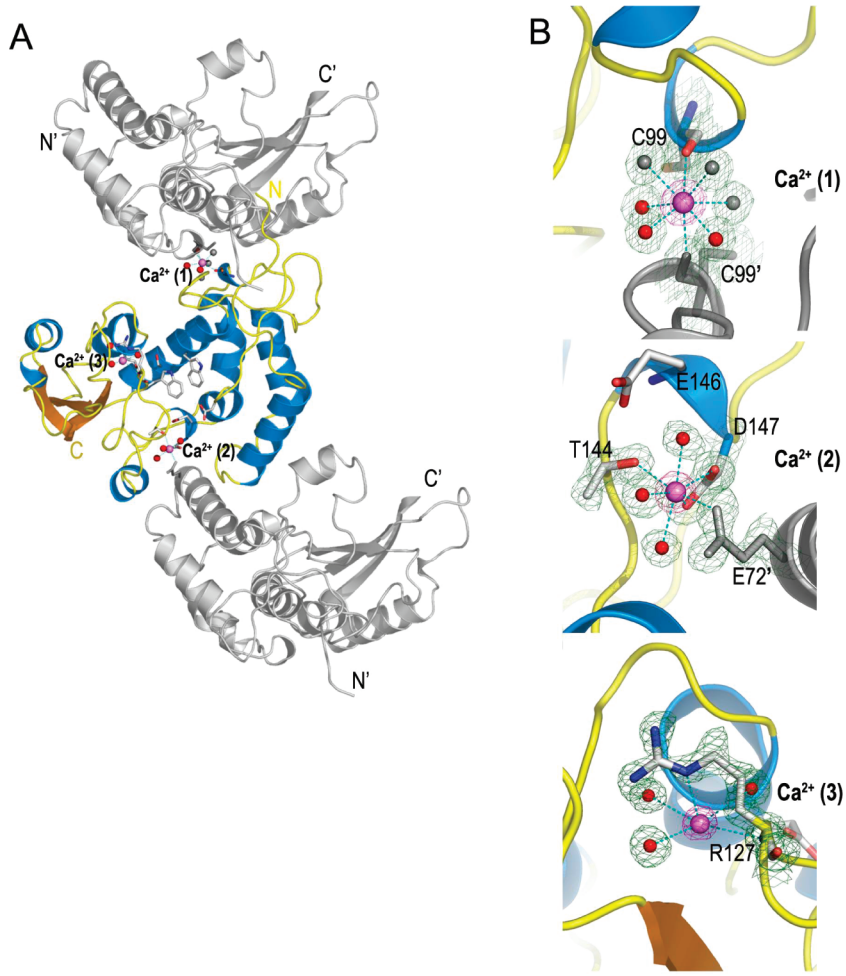


FIGURE 2: Structure of the calcium binding sites. (A) The locations of three bound calcium ions in the calcium-loaded CD38. Two calcium ions, $Ca^{2+}(1)$ and $Ca^{2+}(2)$, are located between the symmetry-related molecules. The third one is bound within the molecule and is close to the catalytic site of CD38. Symmetry-generated molecules are shown as gray ribbons. (B) Structures of the three calcium binding sites. The calcium ions are shown as magenta spheres. Interacting water molecules are shown as red or gray (symmetry-generated) spheres with a smaller size. Protein residues from symmetry-generated molecules are shown as gray sticks.

the "on" structure (cyan) is rotated by 15.5° around the disulfide-linked C119 and C201, the segment can overlap quite well with the corresponding segment in the "off" structure (marine). Therefore, calcium not only induced conformational changes in the two regions but also caused a rigid body rotation of the segment containing residues 201−279.

*The Calcium Loading Sites.* Three calcium ions were identified in the crystallographic asymmetric unit of the calcium-loaded structure. $Ca^{2+}(1)$ and $Ca^{2+}(3)$ were located between the symmetry-related molecules and $Ca^{2+}(2)$ was within the molecule (Figure 2A). $Ca^{2+}(2)$ and $Ca^{2+}(3)$ were close to the active site and $Ca^{2+}(1)$ was on a 2-fold crystallographic axis. The identification of the three calcium ions was based on the $F-F_c$ difference map and their coordination with surrounding protein atoms and solvents (Figure 2B). In a separate control experiment, we crystallized CD38 using a similar crystallization condition but without calcium. The resultant structure was almost identical to the "on" structure, and there were no corresponding electron densities as seen in the "off" structure (data not shown). The involvement of water molecules in the calcium coordination suggests that the binding of calcium to protein is dynamic.

That $Ca^{2+}(1)$ was on the 2-fold axis clearly shows that it played an important role in the intermolecular packing during the crystallization process. Compared with the other two calcium ions, $Ca^{2+}(1)$ is far away from the active site and was not expected to directly regulate the active site function (Figure 2A). In contrast, $Ca^{2+}(2)$ and $Ca^{2+}(3)$ were very close to the active site. Although not directly interacting with the well-established catalytic residues (E226, S193, E146, D155, and W189), they do interact with the regulatory residues, D147 and R127, respectively. Residue R127 has been identified to be involved in substrate binding of NAD and cADPR, and D147 has been linked to the regulation of formation and hydrolysis of cADPR (*12, 15*). Therefore, these two calcium ions are expected to modulate the enzymatic activity.

*Structural Basis for the Enzyme Inactivation.* During the calcium-induced structural transition from the "on" structure to the "off" structure, large structural changes are seen in residues 121−141 near the active site. Figure 3A shows the surface of the active site cleft for the "on" structure with the active site of the "off" structure superimposed as green sticks. The most dramatic difference is that W125 in the "off" structure has now moved into the catalytic pocket and stayed at a position close to W189. The later (W189) together

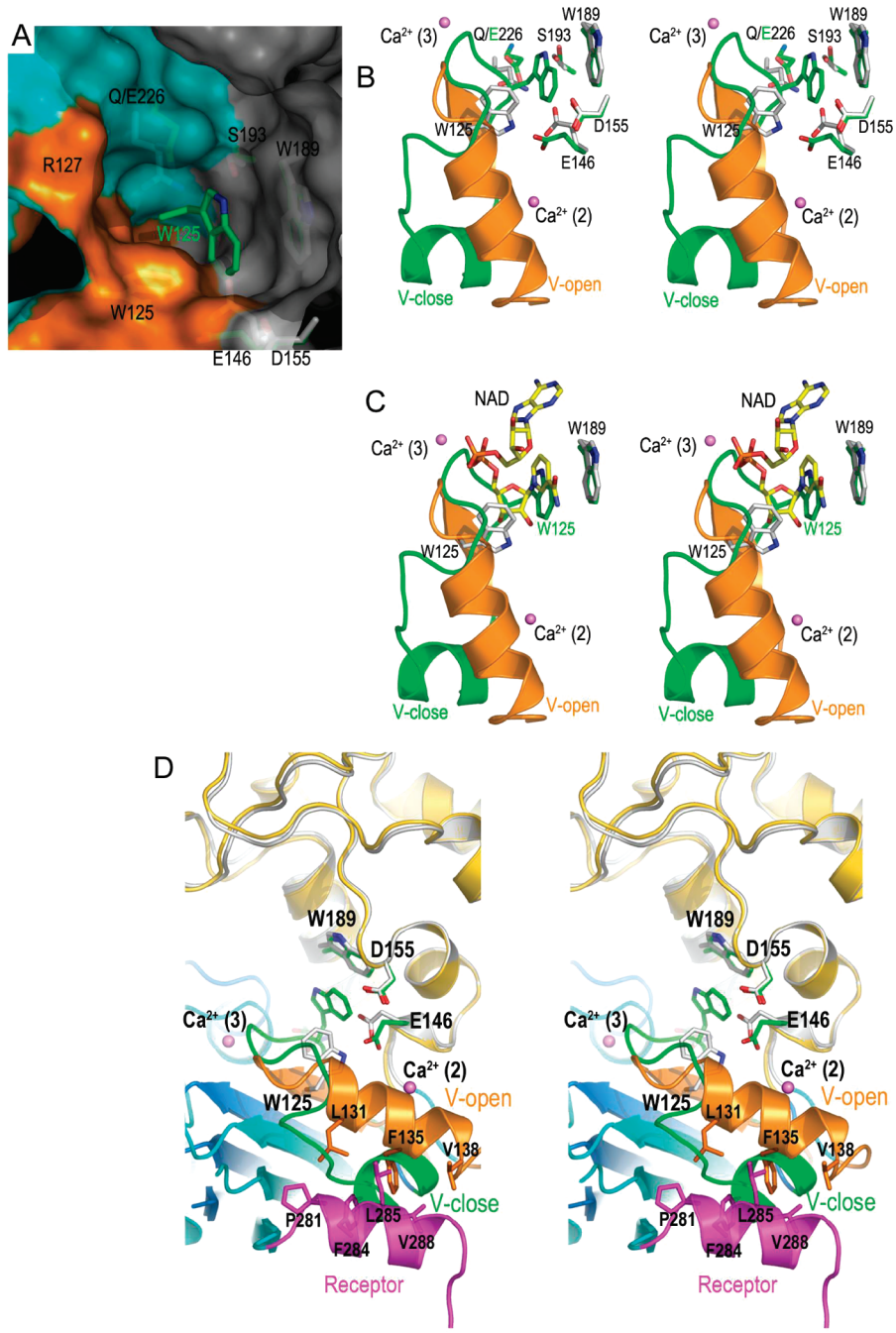


FIGURE 3: Structural basis for the calcium-induced enzyme inactivation. (A) The surface view of the catalytic site of the "on" structure. The corresponding residues in the "off" structure are superimposed as green sticks. The color scheme for the surface is gray for the N-domain, cyan for the C-domain, and orange for the variable region of the C-domain. W125 (green sticks) of the "off" structure moves into the active site of the "on" structure. (B) Structural alignment of the "on" and "off" structures around their active sites. The large movement of W125, which moves from its white position in the "on" structure to the green position in the "off" structure, is shown. The movement of W125 closes the catalytic site, preventing the access of substrates to the catalytic residue E226. The variable region (residues 121−141) of the "off" structure is partially unfolded. (C) Another comparison of the catalytic sites with NAD included. In the "on" structure, the nicotinamide moiety of the bound NAD is parallel to the indole ring of W189. In the "off" structure, loading of calcium induces the movement of W125 to a position overlapping with the nicotinamide moiety of the bound NAD in the "on" structure. (D) Stereo diagram showing the structural basis for conformational coupling between the catalytic site and the receptor region. The disordering of the V-open and receptor regions disrupts the hydrophobic interactions between them, resulting in the movement of the variable region (residues 121−141) from its orange position to green position and the disorder of the receptor region. The overall effect is the movement of W125 toward Trp189. Such movement introduces hydrophobic interactions between two tryptophan indole rings, hides the catalytic residue E226, and thus turns the enzyme off".

with D155, on the other hand, remains in the same position as in the "on" structure (Figure 3B). Concomitant with the translocation of W125 from its white position (Figure 3B) to green position are the side-chain movements for active site residues E226, S193, and E146 (Figure 3B). In the "off" structure, the W125 side-chain ring stacks with the side-chain ring of W189 to form hydrophobic ring−ring interactions. The proximal hydrophobic contact between W125 and W189 actually occludes the catalytic residue E226 from the outside environment and thus prevents binding of the substrate into the active site (Figure 3A,B). As previously shown in the structure of an inactive mutant of CD38 bound

with NAD (*15*), the nicotinamide moiety of the bound NAD is recognized and stabilized by the W189 side chain through hydrophobic interactions. In Figure 3C, the bound NAD in the "on" structure was superimposed with the "off" structure. It can be seen that the W125 side-chain ring in the "off" structure overlaps with the nicotinamide group of the bound NAD and thus blocks its binding to the active site (Figure 3C), leading to inactivation of the enzyme. The close overlapping between W125 and the bound NAD suggests that W125 itself can, in fact, mimic the substrate and occupy the active site through hydrophobic interactions with W189. The translocation of W125 correlates with the unfolding of the α-helix and $\beta$-strand of V-open to a short α-helix and a long loop of V-close (Figure 3C).

To visualize how the loading of calcium can produce the large conformational changes in the C-domain, the "on" and "off" structures were aligned in detail as shown in Figure 3D. In the "on" structure, the receptor and V-open helices are parallel to each other and are mutually stabilized by hydrophobic interactions between them. Loading calcium to site 2 close to the V-open helix (orange, Figure 3D) destabilizes the interaction, allowing the partial unfolding of the V-open helix, which then undergoes conformational transition to form the V-close structure (green, Figure 3D). Concomitantly, the binding of the other calcium at site 3 near the active site then might promote the translocation of W125 to W189, resulting in closure of the active site.

## DISCUSSION

CD38 is a novel protein that has dual functions, both as a signaling enzyme and as a receptor. As an enzyme, it catalyzes the synthesis and hydrolysis of two calcium messenger molecules, cADPR and NAADP (*2, 3, 5*). Its receptorial functions have generally been studied using antibody ligation as a model (*31*). As a receptor, CD38 forms lateral associations with different complexes and has clinical applications in chronic lymphocytic leukemia (CLL) and myeloma (*32*). In CLL patients, CD38 has become a recognized receptor that takes part in the pathway linking growth and survival of the leukemia cells (*33*). For this reason, CD38 has now become a therapeutic target. It has been proposed, however, that the enzymatic and receptorial functions are separate and unrelated (*34*). The results presented in this study provide an alternative possibility with support from a recent identification of two antibodies that can modulate CD38's enzymatic activity (*22*). The conformational coupling between the receptor region and the active site shown here suggests that protein factors interacting with the receptor region can induce changes in the active site and thus regulate the enzymatic activity. Indeed, it has previously been reported that the binding of monoclonal antibodies to CD38 can lead to inhibition of its enzymatic activity (*35*). Likewise, the deletion of part of the receptor region can cause similar inhibition (*20*). The findings that antibodies modulate the enzymatic activity of CD38 may be a stimulus to review a complete panel of the anti-CD38 mAbs now available.

The structural changes induced by calcium are rather dramatic and include partial unraveling of a C-terminal helix (Figures 1 and 3), a rigid body rotation of the segment containing residues 201−279 by more than 15° (Figure 1), and a 5 Å movement of W125 which closes the active site

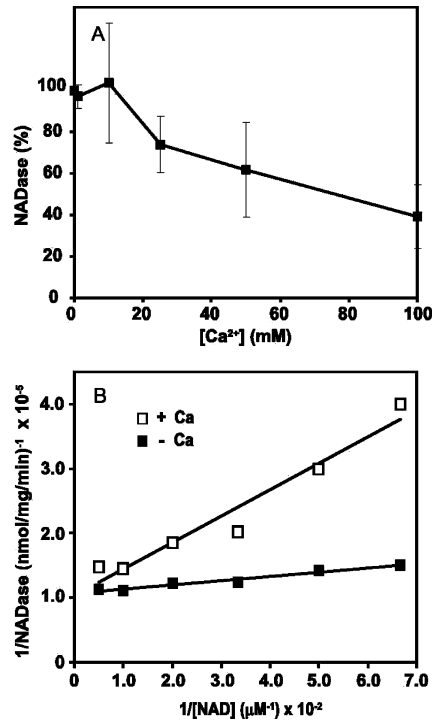


FIGURE 4: Inhibition of the NADase activity of CD38 by calcium. The NADase activity of CD38 was measured as described in the text in the presence of various concentrations of calcium. (A) Calcium inhibits the NADase activity in a concentration-dependent manner. (B) The double reciprocal plot showing that the inhibition by calcium is competitive in nature, decreasing the affinity of CD38 for the substrate NAD. From the plot, the $K_i$ value for calcium was determined to be 19 mM.

pocket (Figure 3). These large structural changes are specific and can be counteracted by the binding of the substrate, NAD, to the catalytic site. As shown in Figure 4A, increasing calcium concentration inhibited the NADase activity of CD38. The inhibition was competitive in nature as shown by the double reciprocal plot (Figure 4B). Thus, at saturating concentrations of NAD, calcium no longer induces inhibition of the enzymatic activity and, by inference, no longer closes the catalytic site. The basis for the competition can be clearly seen in the crystal structure. In the calcium-loaded structure, W125 is shown to have moved to an overlapping position that otherwise would be occupied by the nicotinamide moiety of the bound NAD (Figure 3C). These results show that CD38 is a very flexible molecule and can undergo large structural changes. Indeed, we have previously documented conformational changes associated with substrate binding to the catalytic site of CD38 (*12*), although the changes are not as dramatic as shown here.

It can be argued that the calcium concentrations used in this study are high and may not be physiological. It should be noted that CD38 is expressed on the surface of some cells, such as lymphocytes, and is exposed to millimolar concentrations of calcium. The lateral associations of CD38 with other cell surface molecules (*32*) might synergically work with a low concentration of calcium to inhibit the enzyme. In addition, CLL and myeloma are very good models for environments with high calcium concentration, because the tumor cells reside prevalently in bone marrow, where the calcium levels are higher than in the circulation. The calcium effects are highly magnified in myeloma, where the erosion of the bone increases the amount of calcium in a closed

system. Moreover, during internalization, CD38 is further exposed to acidic pH. We have found that, at acidic pH, the sensitivity of CD38 to calcium is increased (data not shown). Perhaps the main point of this study is not to claim that physiological concentrations of calcium regulate CD38 activity but instead to reveal the dramatic structural changes the molecule exhibits and provide a model for regulation through conformational coupling that can be induced by protein−protein associations with or without calcium.

The results shown in this study have important implications for the regulatory mechanism of this novel signaling enzyme, which until now has been unresolved. Documented evidence has suggested that CD38 can be regulated by phosphorylation, although the actual site of phosphorylation on CD38 has not been demonstrated (*36*). Recently, it has been proposed that agonist-induced internalization can activate CD38, although the exact mechanism has not been delineated (*37*). The flexibility of CD38 demonstrated in this study suggests yet another possibility: that the enzymatic activities of CD38 can be regulated by interaction with other proteins. Clearly, any protein that binds close to the mouth of the active site pocket would inhibit the enzymatic activity by limiting the access of the substrate. As shown in this study, interaction with the C-terminal receptor region can also affect the enzymatic activities through conformational coupling. The results of the closure of the catalytic site by calcium also suggest that calcium may act on surface CD38 by blocking the enzymatic function. A consequential hypothesis is that the block may be followed by recruiting a CD38 internal pool, resulting in the redistribution of CD38 expression, as reported by Munoz et al. (*38*). One would expect that new insights may derive soon from further structural characterization of the multifunctional CD38 protein.

## ACKNOWLEDGMENT

The crystallographic data were collected at the Cornell High Energy Synchrotron Source (CHESS), which is supported by the NSF and NIH, National Institute of General Medical Sciences, under Award DMR-0225180.

## REFERENCES

1. Jackson, D. G., and Bell, J. I. (1990) Isolation of a cDNA encoding the human CD38 (T10) molecule, a cell surface glycoprotein with an unusual discontinuous pattern of expression during lymphocyte differentiation. *J. Immunol. 144*, 2811–2815.
2. Howard, M., Grimaldi, J. C., Bazan, J. F., Lund, F. E., Santos-Argumedo, L., Parkhouse, R. M., Walseth, T. F., and Lee, H. C. (1993) Formation and hydrolysis of cyclic ADP-ribose catalyzed by lymphocyte antigen CD38. *Science 262*, 1056–1059.
3. Aarhus, R., Graeff, R. M., Dickey, D. M., Walseth, T. F., and Lee, H. C. (1995) ADP-ribosyl cyclase and CD38 catalyze the synthesis of a calcium-mobilizing metabolite from NADP. *J. Biol. Chem. 270*, 30327–30333.
4. Lee, H. C. (1997) Mechanisms of calcium signaling by cyclic ADP-ribose and NAADP. *Physiol. Rev. 77*, 1133–1164.
5. Graeff, R., Liu, Q., Kriksunov, I. A., Hao, Q., and Lee, H. C. (2006) Acidic residues at the active sites of CD38 and ADP-ribosyl cyclase determine nicotinic acid adenine dinucleotide phosphate (NAADP) synthesis and hydrolysis activities. *J. Biol. Chem. 281*, 28951–28957.
6. Lee, H. C. (2001) Physiological functions of cyclic ADP-ribose and NAADP as calcium messengers. *Annu. Rev. Pharmacol. Toxicol. 41*, 317–345.
7. Lee, H. C. (2005) Nicotinic acid adenine dinucleotide phosphate (NAADP)-mediated calcium signaling. *J. Biol. Chem. 280*, 33693–33696.
8. Beck, A., Kolisek, M., Bagley, L. A., Fleig, A., and Penner, R. (2006) Nicotinic acid adenine dinucleotide phosphate and cyclic ADP-ribose regulate TRPM2 channels in T lymphocytes. *FASEB J. 20*, 962–964.
9. Perraud, A. L., Fleig, A., Dunn, C. A., Bagley, L. A., Launay, P., Schmitz, C., Stokes, A. J., Zhu, Q., Bessman, M. J., Penner, R., Kinet, J. P., and Scharenberg, A. M. (2001) ADP-ribose gating of the calcium-permeable LTRPC2 channel revealed by Nudix motif homology. *Nature 411*, 595–599.
10. Kolisek, M., Beck, A., Fleig, A., and Penner, R. (2005) Cyclic ADP-ribose and hydrogen peroxide synergize with ADP-ribose in the activation of TRPM2 channels. *Mol. Cell 18*, 61–69.
11. Liu, Q., Kriksunov, I. A., Graeff, R., Munshi, C., Lee, H. C., and Hao, Q. (2005) Crystal structure of human CD38 extracellular domain. *Structure 13*, 1331–1339.
12. Liu, Q., Kriksunov, I. A., Graeff, R., Lee, H. C., and Hao, Q. (2007) Structural basis for formation and hydrolysis of calcium messenger cyclic ADP-ribose by human CD38. *J. Biol. Chem. 282*, 5853–5861.
13. Graeff, R., Munshi, C., Aarhus, R., Johns, M., and Lee, H. C. (2001) A single residue at the active site of CD38 determines its NAD cyclizing and hydrolyzing activities. *J. Biol. Chem. 276*, 12169–12173.
14. Munshi, C., Aarhus, R., Graeff, R., Walseth, T. F., Levitt, D., and Lee, H. C. (2000) Identification of the enzymatic active site of CD38 by site-directed mutagenesis. *J. Biol. Chem. 275*, 21566–21571.
15. Liu, Q., Kriksunov, I. A., Graeff, R., Munshi, C., Lee, H. C., and Hao, Q. (2006) Structural basis for the mechanistic understanding of human CD38-controlled multiple catalysis. *J. Biol. Chem. 281*, 32861–32869.
16. Liu, Q., Kriksunov, I. A., Moreau, C., Graeff, R., Potter, B. V., Lee, H. C., and Hao, Q. (2007) Catalysis-associated conformational changes revealed by human CD38 complexed with a non-hydrolyzable substrate analog. *J. Biol. Chem. 282*, 24825–24832.
17. Ausiello, C. M., Urbani, F., Lande, R., la Sala, A., Di Carlo, B., Baj, G., Surico, N., Hilgers, J., Deaglio, S., Funaro, A., and Malavasi, F. (2000) Functional topography of discrete domains of human CD38. *Tissue Antigens 56*, 539–547.
18. Deaglio, S., Morra, M., Mallone, R., Ausiello, C. M., Prager, E., Garbarino, G., Dianzani, U., Stockinger, H., and Malavasi, F. (1998) Human CD38 (ADP-ribosyl cyclase) is a counter-receptor of CD31, an Ig superfamily member. *J. Immunol. 160*, 395–402.
19. Lande, R., Urbani, F., Di Carlo, B., Sconocchia, G., Deaglio, S., Funaro, A., Malavasi, F., and Ausiello, C. M. (2002) CD38 ligation plays a direct role in the induction of IL-1beta, IL-6, and IL-10 secretion in resting human monocytes. *Cell. Immunol. 220*, 30–38.
20. Hoshino, S., Kukimoto, I., Kontani, K., Inoue, S., Kanda, Y., Malavasi, F., and Katada, T. (1997) Mapping of the catalytic and epitopic sites of human CD38/$NAD^+$ glycohydrolase to a functional domain in the carboxyl terminus. *J. Immunol. 158*, 741–747.
21. Kontani, K., Kukimoto, I., Kanda, Y., Inoue, S., Kishimoto, H., Hoshino, S., Nishina, H., Takahashi, K., Hazeki, O., and Katada, T. (1997) Signal transduction via the CD38/$NAD^+$ glycohydrolase. *Adv. Exp. Med. Biol. 419*, 421–430.
22. Hara-Yokoyama, M., Kimura, T., Kaku, H., Wakiyama, M., Kaitsu, Y., Inoue, M., Kusano, S., Shirouzu, M., Yokoyama, S., Katada, T., Hirabayashi, Y., Takatsu, K., and Yanagishita, M. (2008) Alteration of enzymatic properties of cell-surface antigen CD38 by agonistic anti-CD38 antibodies that prolong B cell survival and induce activation. *Int. Immunopharmacol. 8*, 59–70.
23. Lacapere, J. J., Boulla, G., Lund, F. E., Primack, J., Oppenheimer, N., Schuber, F., and Deterre, P. (2003) Fluorometric studies of ligand-induced conformational changes of CD38. *Biochim. Biophys. Acta 1652*, 17–26.
24. Kukimoto, I., Hoshino, S., Kontani, K., Inageda, K., Nishina, H., Takahashi, K., and Katada, T. (1996) Stimulation of ADP-ribosyl cyclase activity of the cell surface antigen CD38 by zinc ions resulting from inhibition of its $NAD^+$ glycohydrolase activity. *Eur. J. Biochem. 239*, 177–182.
25. Otwinowski, Z., and Minor, W. (1997) Processing of X-ray diffraction data collected in oscillation mode. *Methods Enzymol. 276*, 307–326.
26. Vagin, A., and Teplyakov, A. (2000) An approach to multi-copy search in molecular replacement. *Acta Crystallogr., Sect. D: Biol. Crystallogr. 56*, 1622–1624.
27. Murshudov, G. N., Vagin, A. A., and Dodson, E. J. (1997) Refinement of macromolecular structures by the maximum-

likelihood method. *Acta Crystallogr., Sect. D: Biol. Crystallogr. 53*, 240–255.

28. Morris, R. J., Perrakis, A., and Lamzin, V. S. (2003) ARP/wARP and automatic interpretation of protein electron density maps. *Methods Enzymol. 374*, 229–244.
29. Jones, T. A., Zou, J. Y., Cowan, S. W., and Kjeldgaard, M. (1991) Improved methods for building protein models in electron-density maps and the location of errors in these models. *Acta Crystallogr., Sect. A 47*, 110–119.
30. Graeff, R., and Lee, H. C. (2002) A novel cycling assay for nicotinic acid-adenine dinucleotide phosphate with nanomolar sensitivity. *Biochem. J. 367*, 163–168.
31. Malavasi, F., Funaro, A., Alessio, M., DeMonte, L. B., Ausiello, C. M., Dianzani, U., Lanza, F., Magrini, E., Momo, M., and Roggero, S. (1992) CD38: a multi-lineage cell activation molecule with a split personality. *Int. J. Clin. Lab. Res. 22*, 73–80.
32. Malavasi, F., Deaglio, S., Funaro, A., Ferrero, E., Horenstein, A. L., Ortolan, E., Vaisitti, T., and Aydin, S. (2008) Evolution and function of the ADP ribosyl cyclase/CD38 gene family in physiology and pathology. *Physiol. Rev. 88*, 841–886.
33. Deaglio, S., Vaisitti, T., Bergui, L., Bonello, L., Horenstein, A. L., Tamagnone, L., Boumsell, L., and Malavasi, F. (2005) CD38 and CD100 lead a network of surface receptors relaying positive signals for B-CLL growth and survival. *Blood 105*, 3042–3050.
34. Lund, F. E., Muller-Steffner, H. M., Yu, N., Stout, C. D., Schuber, F., and Howard, M. C. (1999) CD38 signaling in B lymphocytes is controlled by its ectodomain but occurs independently of enzymatically generated ADP-ribose or cyclic ADP-ribose. *J. Immunol. 162*, 2693–2702.
35. Adebanjo, O. A., Anandatheerthavarada, H. K., Koval, A. P., Moonga, B. S., Biswas, G., Sun, L., Sodam, B. R., Bevis, P. J., Huang, C. L., Epstein, S., Lai, F. A., Avadhani, N. G., and Zaidi, M. (1999) A new function for CD38/ADP-ribosyl cyclase in nuclear $Ca^{2+}$ homeostasis. *Nat. Cell Biol. 1*, 409–414.
36. Willmott, N., Sethi, J. K., Walseth, T. F., Lee, H. C., White, A. M., and Galione, A. (1996) Nitric oxide-induced mobilization of intracellular calcium via the cyclic ADP-ribose signaling pathway. *J. Biol. Chem. 271*, 3699–3705.
37. Rah, S. Y., Park, K. H., Nam, T. S., Kim, S. J., Kim, H., Im, M. J., and Kim, U. H. (2007) Association of CD38 with nonmuscle myosin heavy chain IIA and Lck is essential for the internalization and activation of CD38. *J. Biol. Chem. 282*, 5653–5660.
38. Munoz, P., Mittelbrunn, M., de la Fuente, H., Perez-Martinez, M., Garcia-Perez, A., Ariza-Veguillas, A., Malavasi, F., Zubiaur, M., Sanchez-Madrid, F., and Sancho, J. (2008) Antigen-induced clustering of surface CD38 and recruitment of intracellular CD38 to the immunologic synapse. *Blood 111*, 3653–3664.

BI801642Q